Paleoceanography

Supporting Information for

Antarctic Intermediate Water circulation in the South Atlantic over the past 25,000 years

Jacob N. W. Howe,[1*] Alexander M. Piotrowski,[1] Delia W. Oppo,[2] Kuo-Fang Huang,[2,3] Stefan Mulitza,[4] Cristiano M. Chiessi,[5] Jurek Blusztajn[2]

[1]Department of Earth Sciences, University of Cambridge, Cambridge, CB2 3EQ, UK

[2]Department of Geology and Geophysics, Woods Hole Oceanographic Institution, Woods Hole, Massachusetts, 02543, USA

[3]Institute of Earth Sciences, Academia Sinica, Taipei, 11529, Taiwan

[4]MARUM - Center for Marine Environmental Sciences, University of Bremen, Leobener Strasse, D-28359 Bremen, Germany

[5]School of Arts, Sciences and Humanities, University of São Paulo,

Av. Arlindo Bettio 1000, CEP03828-000 São Paulo SP, Brazil

Contents of this file

Introduction

This supplement includes additional data measured on cores from the Demerara Rise with the methods detailed in Text S1, an extended discussion in Text S2, and the results presented in Figures S1 to S3. All data measured in this work is then listed in Tables S1 to S7 along with external errors (2σ).

Text S1. Supplementary methods:

Rare earth element analysis

Rare Earth Element (REE) concentrations were determined by a Thermo-Fisher Element XR High-Resolution Inductively Coupled Plasma Mass Spectrometer (HR-ICP-MS) in the institute of Earth Sciences, Academia Sinica, Taiwan. In order to enhance sensitivity and reduce polyatomic interferences (e.g. oxide/hydride formations), a Cetac Aridus II desolvation system was applied to measure REE concentrations. Each sample containing 20-40 ppm Ca was directly measured on Element XR. After blank, drift and BaO corrections, signal intensities were converted to concentrations using a series of external matrix-matched synthetic standards, which were prepared from NIST traceable High Purity Standards (HPS) solutions and calibrated by standard addition. Replicated measurements on in-house standards with REE/Ca ratios of 1-200 nmol/mol show that the long-term reproducibility for the REE is better than 5% (2 RSD).

Detrital fraction

The detrital fraction of KNR197-3-25GGC and KNR197-3-9GGC were prepared for analysis following the method of *Bayon et al.* [2002]. In short, ~100 mg of sediment was decarbonated using 10% acetic acid. Samples were then leached with 1 M hydroxylamine hydrochloride in 25% acetic acid for 3 hours on a hot plate at 90°C to remove ferromanganese oxides. The detrital fraction was then dissolved using a 4:1 mixture of HF:$HClO_4$ before finally being taken up in 6M HCl for processing and analysis of neodymium isotopic composition at Woods Hole Oceanographic Institution as described in the main text.

Test S2. Supplementary Discussion:

The new detrital neodymium isotope records of the Demerara Rise cores KNR197-3-25GGC (hereafter 25GGC) and KNR197-3-9GGC (hereafter 9GGC) collected in this work are very similar to the previously published foraminiferal ε_{Nd} records from the same cores (Supplementary Figure 2; [*Huang et al.*, 2014]). In particular the detrital records show excursions to less radiogenic values during the Northern Hemisphere cold periods Heinrich Stadial 1 and the Younger Dryas. This contrasts with the detrital and foraminiferal ε_{Nd} data from the core KNR197-3-46CDH (46CCDH hereafter; Supplementary Figure 2) - which lies at an intermediate depth to these two cores - that showed no correlation between the detrital and foraminiferal values (Supplementary information of *Huang et al.* [2014]). The similarity of the data from the detrital and authigenic phase Nd isotopes in 25GGC and 9GGC suggests that the excursions observed in the foraminiferal Nd isotopes during the Northern Hemisphere cold periods could be due to changes in the detrital composition overprinting the foraminiferal signature.

There is, however, evidence to suggest that the foraminiferal records must be largely reflective of past changes in the ε_{Nd} of bottom water bathing the intermediate depth Demerara Rise. Firstly the rare earth element profiles of the uncleaned foraminifera from both cores (Supplementary Figure 3) show no change in shape between the Younger Dryas and Heinrich Stadial 1 aged samples and Holocene, Bølling-Allerød and Last Glacial Maximum aged samples. All five samples from each core show the middle rare earth element bulge typical of the fractionation of rare earth elements from seawater into the ferromanganese coatings of foraminifera [*Kraft et al.*, 2013]. This indicates that the unradiogenic excursions observed during the Northern Hemisphere cold periods in the foraminiferal ε_{Nd} records of 25GGC and 9GGC are unlikely to be caused by diagenetic overprinting of the ferromanganese coatings in the sediment as the REE profiles are not consistent with a detrital REE pattern [*Gutjahr et al.*, 2007].

Furthermore, the lack of correlation between the foraminiferal and detrital values of 46CDH argues against a simple detrital control of the foraminiferal record of that core. In particular there is no noteworthy change in the detrital ε_{Nd} of 46CDH between the LGM and HS1 whereas there is a 2.5 epsilon unit shift to less radiogenic values in the foraminiferal record of 46CDH across the same transition (Supplementary Figure 2). This indicates that the shift in the foraminiferal record must reflect a change in bottom water ε_{Nd}. Given the proximity of 25GGC and 9GGC to 46CDH it follows that the similar shifts observed in the foraminiferal ε_{Nd} records in the former cores reflect the same change in bottom water composition. This conclusion reveals that the detrital composition modifying pore waters and diagenetically overprinting the foraminiferal ferromanaganese coatings cannot be the dominant control on the foraminiferal records of all three sites.

The exclusion of pore water processes controlling the foraminiferal records implies that the records represent real changes in the past ε_{Nd} of seawater bathing the intermediate depth Demerara Rise. These changes could reflect changes in water mass mixing; however, they could also reflect either changes in the composition of water mass end-members during these millennial scale climate perturbations or else localised signals of modified seawater. Intermediate depth corals from the North Atlantic [*van de Flierdt et al.*, 2006; *Wilson et al.*, 2014] do not show ε_{Nd} values less radiogenic than the composition of modern NADW (Figure 4). This observation argues against the signal representing a change in the ε_{Nd} of the northern-sourced endmember. Meanwhile the records from the southern Brazil margin presented in this work show no indication of changes in the composition of AAIW during HS1 and the YD (Figure 3), ruling out changes in the southern-sourced water mass.

It is more difficult to discount the possibility that that unradiogenic sediment, potentially from the Guiana Shield [*White et al.*, 1985; *McDaniel et al.*, 1997], transported to the Demerara Rise may have relabelled seawater neodymium isotopes in this region via boundary exchange [*Lacan and Jeandel*, 2005]. The inference of slower circulation in the Atlantic during these Northern Hemisphere cold events from $^{231}Pa/^{230}Th$ measurements [*McManus et al.*, 2004; *Bradtmiller et al.*, 2014] would allow more time for the exchange of neodymium to occur when bottom waters interacted with the margins [*Lacan and Jeandel*, 2005], or whilst sediment particles descended through the water column [*Siddall et al.*, 2008]. A similar phenomenon was observed during the Last Glacial Maximum in the northern Northeast Atlantic [*Roberts and Piotrowski*, 2015]. Although this possibility precludes certainty in the water mass mixing proportions at these Demerara Rise sites during HS1 and the YD, the aforementioned North Atlantic coral records and the new southern Brazil margin records presented in this work do not appear to have any similar indications of local modification of seawater by detrital material during these time intervals. As a result we conclude that the direction of change of the Demerara Rise foraminiferal records during HS1 and the YD is likely to reflect changes in water mass mixing supporting the conclusions of *Huang et al.* [2014]. However, we note that the possibility of the seawater signal being slightly modified by local sediment during those Northern Hemisphere cold periods cannot be fully discounted which is why we advise caution when interpreting the absolute values. Notwithstanding these limitations of the Demerara Rise records, the interpretation of the southern Brazil margin records presented in this work as providing no indication for a greater influence of AAIW in the intermediate depth South Atlantic during HS1 and the YD remains robust.

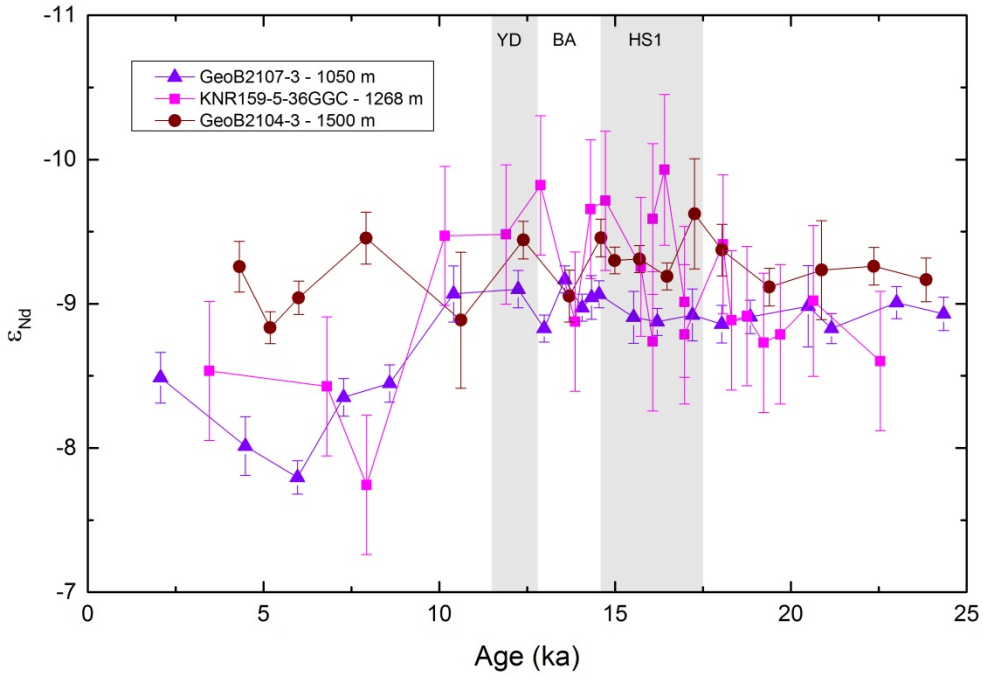

Figure S1. ε_{Nd} of uncleaned foraminifera from cores GeoB2107-3 (purple triangles; 27.2°S, 46.5°W, 1050 m), KNR159-5-36GGC (pink squares; 27.5°S, 46.5°W, 1268 m) and GeoB2104-3 (burgundy circles; 27.3°S, 46.4°W, 1500 m). Error bars give the 2σ external error of each measurement. Climate periods labelled are the Younger Dryas (YD), Bølling-Allerød (BA) and Heinrich Stadial 1 (HS1).

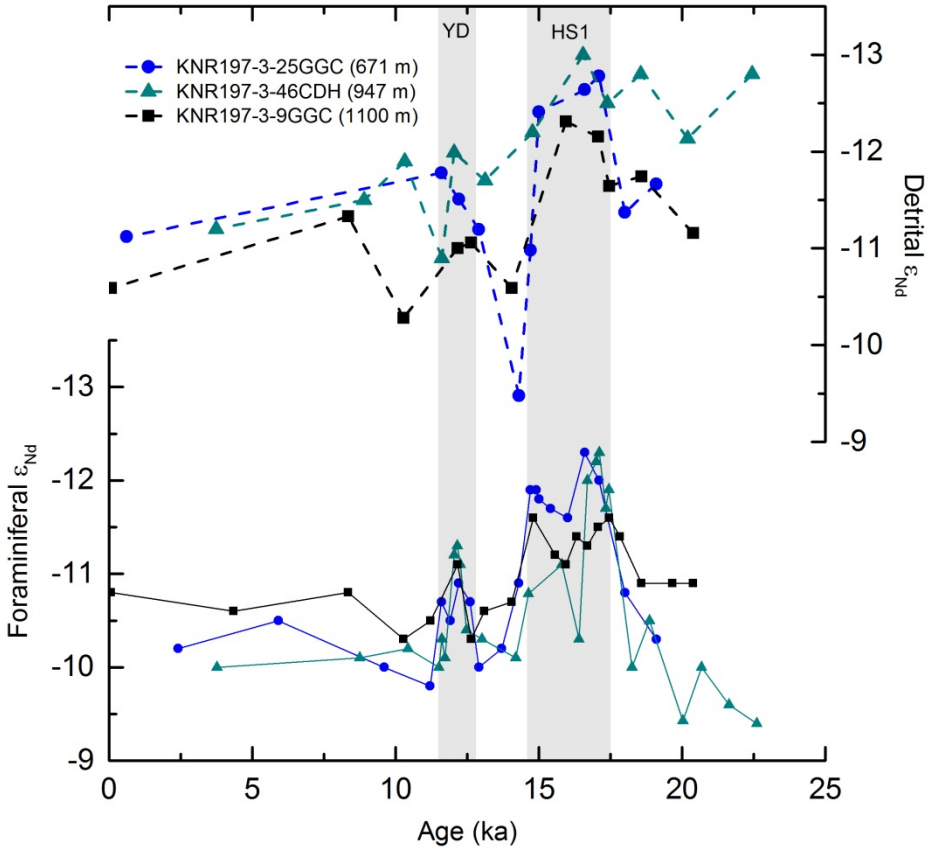

Figure S2. Detrital (dashed lines) and foraminiferal (solid lines) ε_{Nd} values of KNR197-3-25GGC (7.7°N, 53.8°W; 671 m), KNR197-3-46CDH (7.8°N, 53.7°W; 947 m) and KNR197-3-9GGC (7.9°N, 53.6°W; 1100 m). Detrital values for KNR197-3-25GGC and KNR197-3-9GGC were measured in this work, all other data comes from *Huang et al.* [2014]. Northern Hemisphere cold periods labelled are the Younger Dryas (YD) and Heinrich Stadial 1 (HS1).

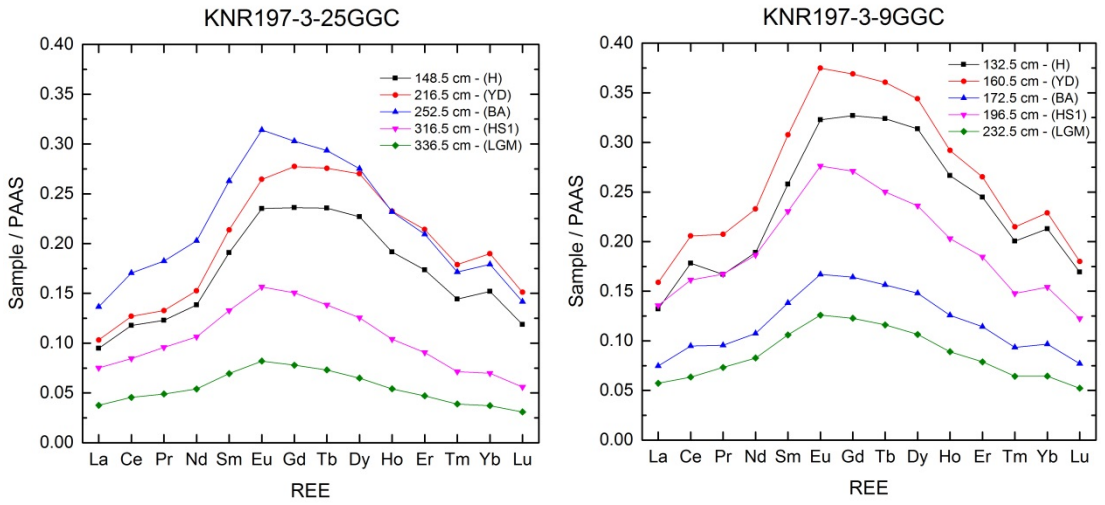

Figure S3. Rare earth element (REE) profiles of uncleaned planktic foraminifera from KNR197-3-25GGC (7.7°N, 53.8°W; 671 m) and KNR197-3-9GGC (7.9°N, 53.6°W; 1100 m). All concentrations are in ppm calcite normalised to Post Archean Australian Shale (PAAS) [*Taylor and McLennan*, 1985]. Curves are labelled with their corresponding depths from within each core along with the climate period they are dated within including the Holocene (H), Younger Dryas (YD), Bølling-Allerød (BA), Heinrich Stadial 1 (HS1) and the Last Glacial Maximum (LGM).

Table S1. ε_{Nd} data of planktic foraminifera, decarbonated leachates and the detrital fraction of GeoB2107-3.

Depth (cm)	Age (ka)	$^{143}Nd/^{144}Nd$ (foraminifera)	ε_{Nd} (foraminifera)	2σ	ε_{Nd} (leachate)	$^{143}Nd/^{144}Nd$ (leachate)	2σ	$^{143}Nd/^{144}Nd$ (detrital)	ε_{Nd} (detrital)	2σ
9	2.1	0.512203	-8.49	0.18	0.512305	-6.5	0.27	0.512145	-9.62	0.09
25	4.5	0.512227	-8.01	0.2	0.512350	-5.62	0.3			
35	6	0.512238	-7.8	0.12						
45	7.3	0.512210	-8.35	0.13						
55	8.6	0.512205	-8.45	0.13						
65	10.4	0.512173	-9.07	0.19	0.512328	-6.05	0.24	0.512175	-9.04	0.09
70	12.2	0.512171	-9.1	0.13						
72	13	0.512185	-8.83	0.17						
76.5	13.6	0.512168	-9.17	0.16						
86	14.1	0.512178	-8.97	0.14						
91	14.3	0.512175	-9.04	0.15						
95	14.5	0.512173	-9.07	0.14						
105.5	15.5	0.512181	-8.91	0.18						
110	16.2	0.512183	-8.87	0.09						
116	17.2	0.512181	-8.92	0.18						
121	18	0.512184	-8.86	0.13						
126	18.8	0.512181	-8.91	0.2						
136	20.5	0.512178	-8.98	0.28						
140	21.2	0.512185	-8.83	0.1	0.512351	-5.59	0.24	0.512130	-9.91	0.17
156	23	0.512176	-9.01	0.11						
166	24.3	0.51218	-8.93	0.12						

Table S2. ε_{Nd} data of planktic foraminifera from KNR159-5-36GGC.

Depth (cm)	Age (ka)	$^{143}Nd/^{144}Nd$ (foraminifera)	ε_{Nd} (foraminifera)	2σ
10	3.5	0.512200	-8.53	0.48
40	6.8	0.512206	-8.43	0.48
48	7.9	0.512241	-7.74	0.48
64	10.2	0.512153	-9.47	0.48
70.5	11.9	0.512152	-9.48	0.48
78.5	12.9	0.512134	-9.82	0.48
86.5	13.9	0.512183	-8.88	0.48
94.5	14.3	0.512143	-9.66	0.48
102.5	14.7	0.512140	-9.71	0.48
110.5	15.7	0.512164	-9.26	0.48
118.5	16.1	0.512190	-8.74	0.48
118.5	16.1	0.512147	-9.59	0.52
126.5	16.4	0.512129	-9.93	0.52
134.5	17.0	0.512176	-9.01	0.52
134.5	17.0	0.512187	-8.79	0.48
142.5	18.1	0.512155	-9.41	0.48
150.5	18.3	0.512183	-8.89	0.48
158.5	18.8	0.512181	-8.91	0.48
166.5	19.2	0.512190	-8.73	0.48
174.5	19.7	0.512187	-8.79	0.48
182.5	20.6	0.512176	-9.02	0.52
190.5	22.5	0.512197	-8.60	0.48

Table S3. εNd data of planktic foraminifera, decarbonated leachates and the detrital fraction of GeoB2104-3.

Depth (cm)	Age (ka)	$^{143}Nd/^{144}Nd$ (foraminifera)	ε_{Nd} (foraminifera)	2σ	$^{143}Nd/^{144}Nd$ (leachate)	ε_{Nd} (leachate)	2σ	$^{143}Nd/^{144}Nd$ (detrital)	ε_{Nd} (detrital)	2σ
5	4.3	0.512163	-9.26	0.18	0.512258	-7.41	0.25	0.512127	-9.96	0.12
19	5.2	0.512185	-8.83	0.11	0.512283	-6.92	0.25			
32	6	0.512175	-9.04	0.12						
44	7.9	0.512153	-9.46	0.18						
60	10.6	0.512182	-8.89	0.47	0.512293	-6.73	0.25	0.512125	-10.01	0.22
65	12.4	0.512154	-9.44	0.16						
70	13.7	0.512174	-9.05	0.18						
75	14.6	0.512153	-9.46	0.13						
80	15	0.512161	-9.3	0.14						
89	15.7	0.512161	-9.31	0.14						
99	16.5	0.512167	-9.19	0.16						
109	17.3	0.512145	-9.62	0.38						
119	18	0.512158	-9.37	0.18						
129	19.4	0.512170	-9.12	0.13						
139	20.9	0.512165	-9.23	0.34	0.512329	-6.03	0.24	0.512115	-10.2	0.18
149	22.4	0.512163	-9.26	0.13						
159	23.8	0.512168	-9.17	0.15						

Table S4. ε_{Nd} data of the detrital fraction of KNR197-3-25GGC.

Depth (cm)	Age (ka)	$^{143}Nd/^{144}Nd$	ε_{Nd}	2σ
0.5	0.6	0.512068	-11.12	0.3
204.5	11.6	0.512034	-11.78	0.3
220.5	12.2	0.512048	-11.51	0.3
236.5	12.9	0.512064	-11.20	0.3
268.5	14.3	0.512152	-9.48	0.3
276.5	14.7	0.512075	-10.98	0.3
284.5	15.0	0.512002	-12.41	0.3
312.5	16.6	0.511990	-12.64	0.3
320.5	17.1	0.511983	-12.78	0.3
332.5	18.0	0.512055	-11.37	0.3
348.5	19.1	0.512040	-11.67	0.3

Table S5. ε_{Nd} data of the detrital fraction of KNR197-3-9GGC.

Depth (cm)	Age (ka)	$^{143}Nd/^{144}Nd$	ε_{Nd}	2σ
0.5	0.1	0.512095	-10.59	0.3
88.5	8.4	0.512057	-11.33	0.3
140.5	10.3	0.512111	-10.28	0.3
156.5	12.2	0.512074	-11.00	0.3
160.5	12.6	0.512071	-11.06	0.3
172.5	14.1	0.512095	-10.59	0.3
192.5	15.9	0.512007	-12.31	0.3
204.5	17.1	0.512015	-12.15	0.3
208.5	17.5	0.512041	-11.65	0.3
220.5	18.6	0.512036	-11.74	0.3
240.5	20.4	0.512066	-11.16	0.3

Table S6. Rare earth element concentrations of uncleaned planktic foraminifera from KNR197-3-25GGC. All concentrations are in ppm calcite normalised to Post Archean Australian Shale (PAAS) [*Taylor and McLennan*, 1985].

Depth (cm)	La	Ce	Pr	Nd	Sm	Eu	Gd	Tb	Dy	Ho	Er	Tm	Yb	Lu
148.5	0.09	0.12	0.12	0.14	0.19	0.24	0.24	0.24	0.23	0.19	0.17	0.14	0.15	0.12
216.5	0.10	0.13	0.13	0.15	0.21	0.26	0.28	0.28	0.27	0.23	0.21	0.18	0.19	0.15
252.5	0.14	0.17	0.18	0.20	0.26	0.31	0.30	0.29	0.28	0.23	0.21	0.17	0.18	0.14
316.5	0.08	0.08	0.10	0.11	0.13	0.16	0.15	0.14	0.13	0.10	0.09	0.07	0.07	0.06
336.5	0.04	0.05	0.05	0.05	0.07	0.08	0.08	0.07	0.06	0.05	0.05	0.04	0.04	0.03

Table S7. Rare earth element concentrations of uncleaned planktic foraminifera from KNR197-3-9GGC. All concentrations are in ppm calcite normalised to Post Archean Australian Shale (PAAS) [*Taylor and McLennan*, 1985].

Depth (cm)	La	Ce	Pr	Nd	Sm	Eu	Gd	Tb	Dy	Ho	Er	Tm	Yb	Lu
132.5	0.13	0.18	0.17	0.19	0.26	0.32	0.33	0.32	0.31	0.27	0.24	0.20	0.21	0.17
160.5	0.16	0.21	0.21	0.23	0.31	0.37	0.37	0.36	0.34	0.29	0.27	0.21	0.23	0.18
172.5	0.07	0.09	0.10	0.11	0.14	0.17	0.16	0.16	0.15	0.13	0.11	0.09	0.10	0.08
196.5	0.14	0.16	0.17	0.19	0.23	0.28	0.27	0.25	0.24	0.20	0.18	0.15	0.15	0.12
232.5	0.06	0.06	0.07	0.08	0.11	0.13	0.12	0.12	0.11	0.09	0.08	0.06	0.06	0.05